Supplementary Material

for

Aptamer-Based Fluorescence Polarization Assay for Separation-Free Exosome Quantification

Zhen Zhang[a,*], Chuanhao Tang[b], Libo Zhao[c], Li Xu[a], Wei Zhou[a,d], Zaizai Dong[a,d], Yuqing Yang[c], Qiqi Xie[c], and Xiaohong Fang[a,d,*]

[a] CAS Key Laboratory of Molecular Nanostructure and Nanotechnology, Beijing National Research Center for Molecular Sciences,
CAS Research/Education Center for Excellence in Molecule Science, Institute of Chemistry, Chinese Academy of Sciences, Beijing 100190, China

[b] Department of Medical Oncology, Peking University International Hospital, Beijing 102206, P. R. China

[c] Echo Biotech Co. Ltd, Beijing 102206, P. R. China

[d] University of Chinese Academy of Sciences, Beijing 100049, P. R. China

* Corresponding authors. *E-mail:* xfang@iccas.ac.cn. zhangzhen@iccas.ac.cn

Equation for fluorescence polarization calculation

$$\frac{1}{P} = \frac{1}{P_0} + \left(\frac{1}{P_0} - \frac{1}{3}\right)\frac{RT\tau}{V\eta}$$ Equation S1

Fluorescence polarization is a ratio, defined as the difference between linearly polarized component of emission divided by the total light intensity. [1] The *P* value is sensitive to changes in the rotational motion of fluorescently labeled molecules. It can be calculated by the Perrin equation (Equation S1), where τ is the fluorescence lifetime, η is the viscosity of the solution, *T* is the temperature in Kelvin, *R* is the gas constant, *V* is the volume of the rotating unit, and P_0 is the limiting polarization. The *P* value of a fluorophore is proportional to its rotational relaxation time, which in turn depends upon the molecular volume/mass. If a molecule is small it will rotate faster and hence will have a smaller *P* value. Conversely, larger molecules will have larger *P* value because of their slow rotation.[2]

Supporting figures

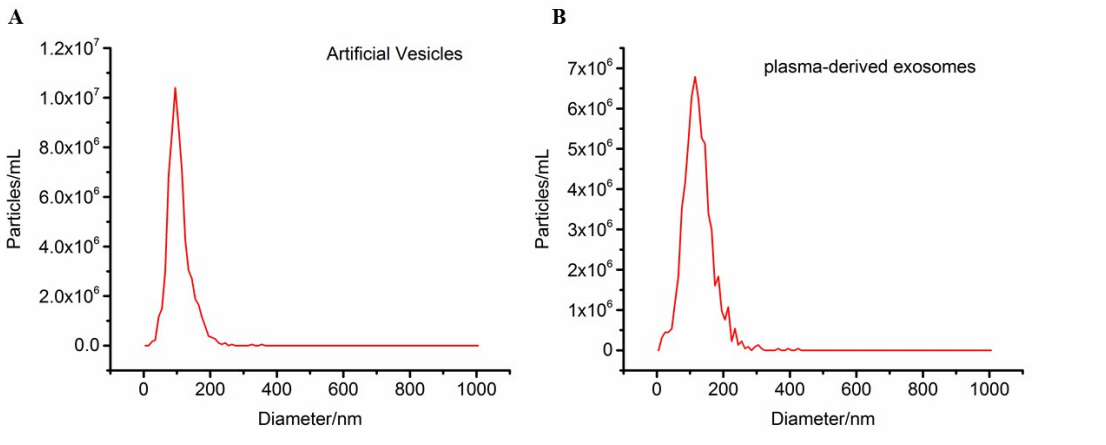

Fig. S1. Size distribution of exosomes by Nanoparticle Tracking Analysis (NTA). (A) artificial exosomes; (B) human plasma-derived exosomes. All the exosomes have uniform sizes at around 100 nm.

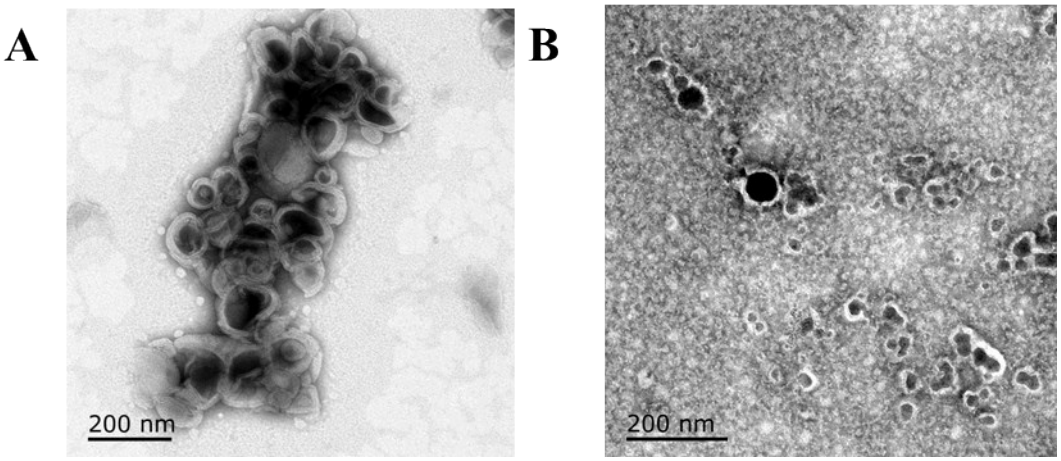

Fig. S2. Transmission electron microscopy images of exosomes. (A) artificial exosomes; (B) human plasma-derived exosomes. Scale bar: 200 nm.

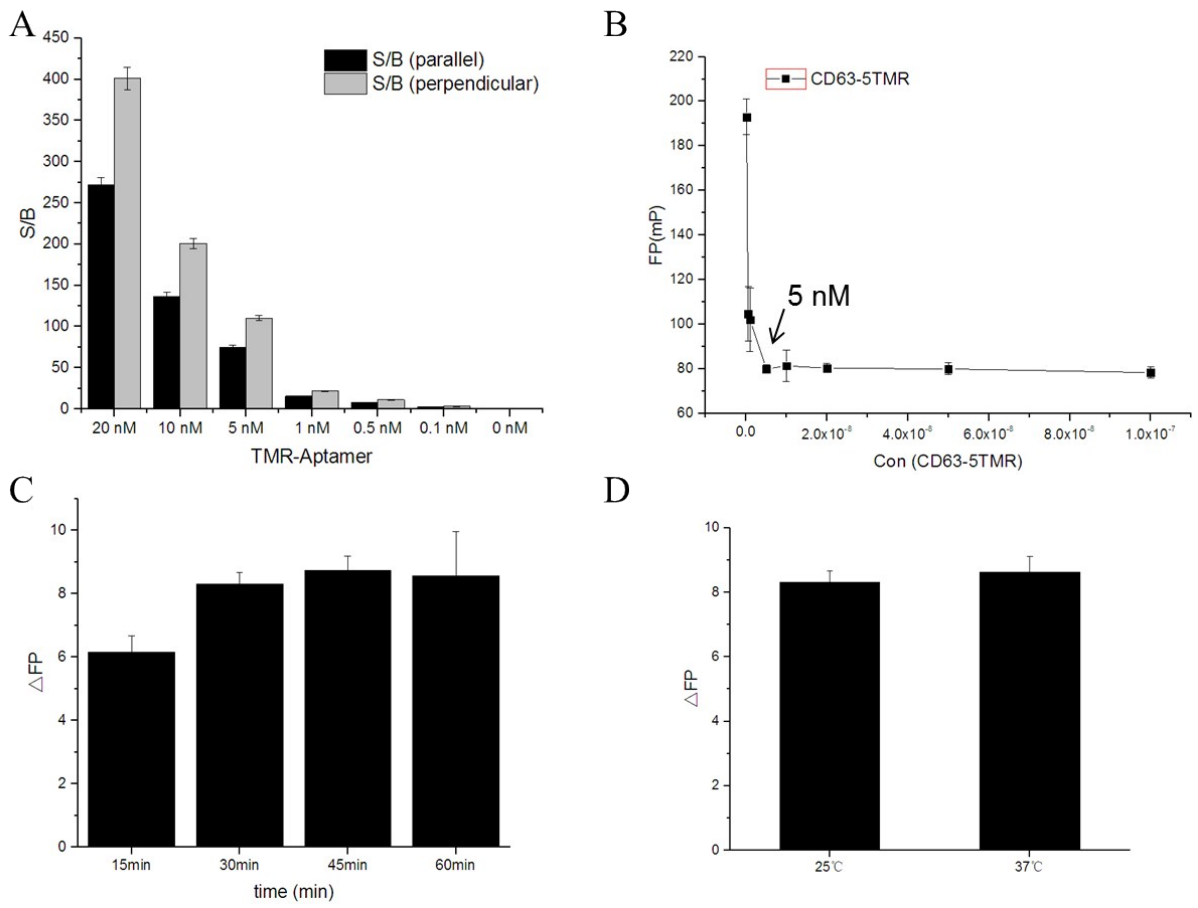

Fig. S3. Optimization of experiment conditions for the AFPExo assay. (A)Parallel/perpendicular fluorescence intensity signal to background ratio of TMR-aptamer at different concentrations; (B) Fluorescence polarization of TMR-aptamer at different concentrations; (C) Effect of incubation time on FP change; (D) Effect of incubation temperature on FP change.

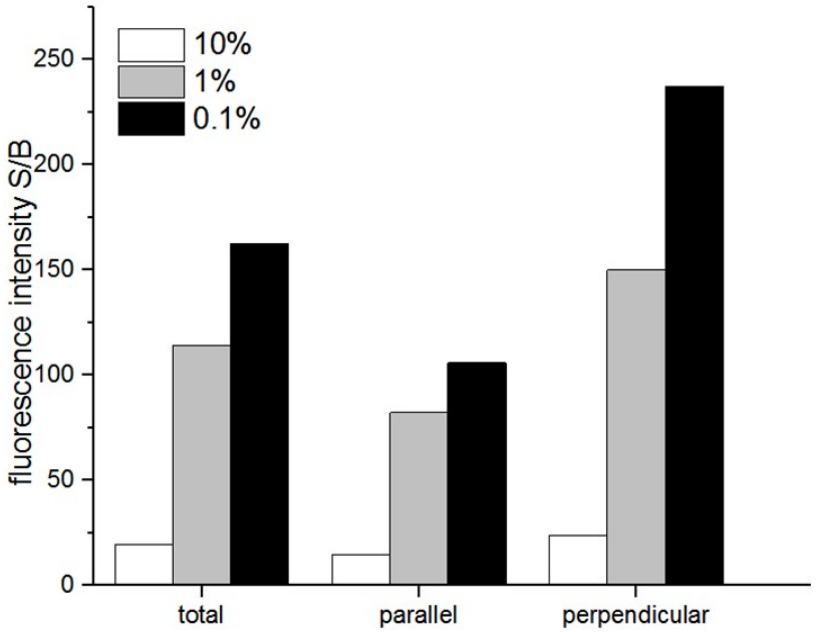

Fig. S4. Evaluation of the fluorescence intensity signal to background ratio of 5nM aptamer in 10%, 1%, 0.1% human serum. Total: total fluorescence intensity; Parallel: the fluorescence intensity parallel to the excitation plane; Perpendicular: the fluorescence intensity perpendicular to the excitation plane.

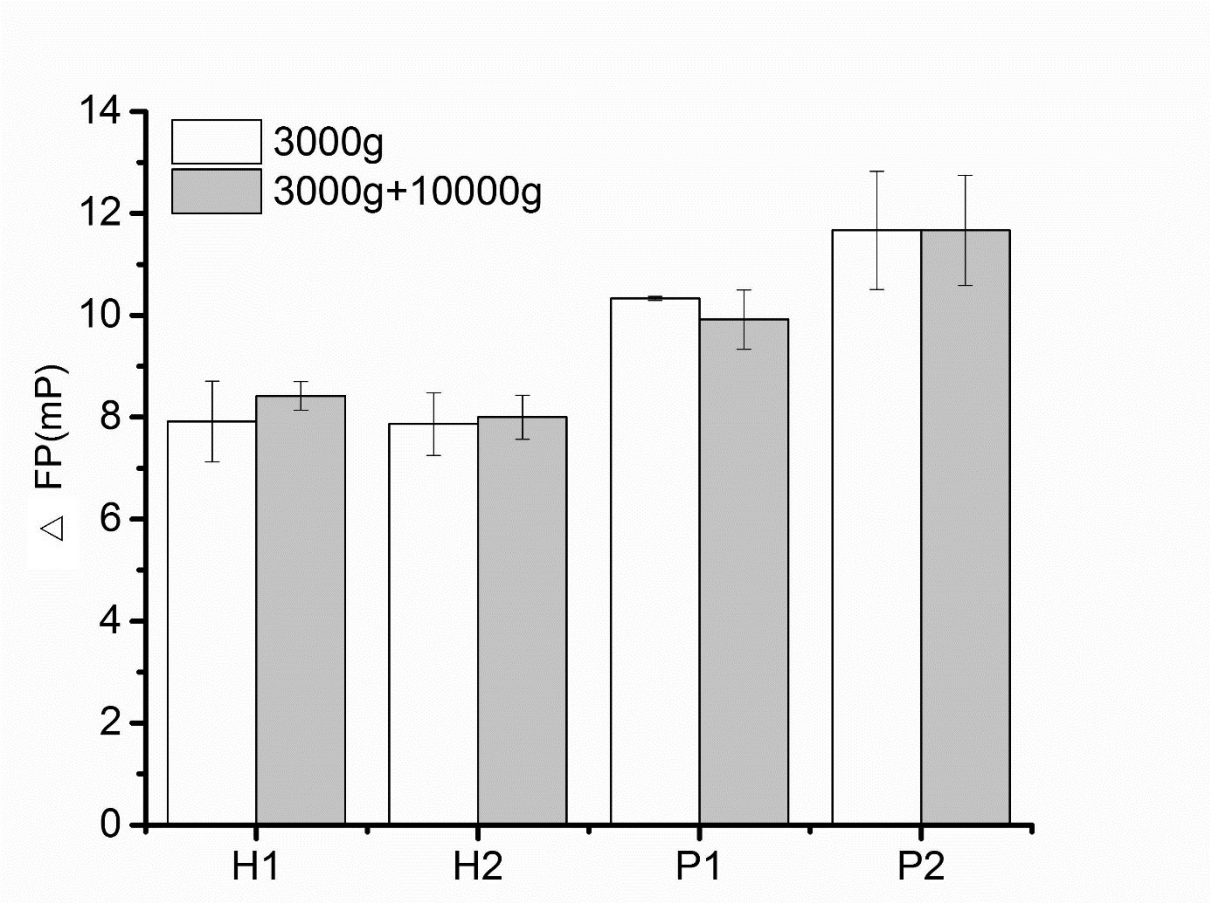

Fig. S5. The fluorescence polarization changes of clinical plasma samples treated with different centrifugation speeds. The clinical plasma from four donors (two healthy donors (H1,H2) and two cancer patients (P1, P2) was exposed to a two-step centrifugation. The samples were centrifuged at 3000 g to prepare platelet-poor plasma (PPP)/ platelet-free plasma (PFP) which eliminate the whole blood cells and platelet. Then, two-third of the PPP/PFP was transferred to new tubes and centrifuged at 10000 g to remove the whole cell debris. Finally, the supernatant was used as two-step centrifuged plasma. AFPExo assay was used to detect exosomes in the PPP/PFP plasma (3000g) and two-step centrifuged plasma (3000 g+ 10000 g). The error bars represent the standard deviations from three repetitive measurements.

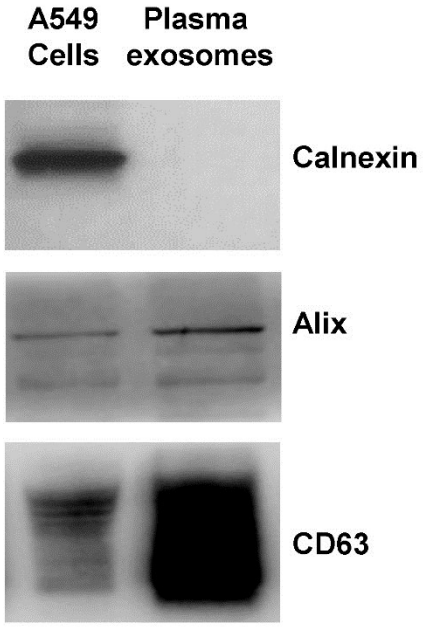

Fig. S6. Western blot analysis of the marker proteins, Calnexin, Alix, CD63 and TSG101, in A549 cells and plasma exosomes.

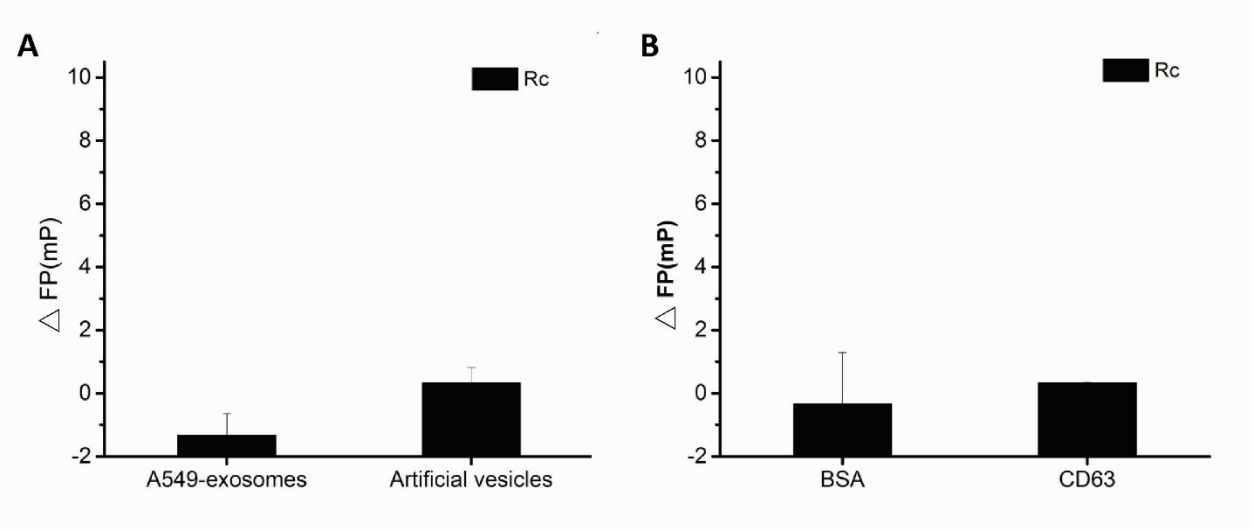

Fig. S7. The fluorescence polarization change of 5 nM TMR-Rc after incubation with 5×10^5 particles/μL of A549-exosomes or artificial vesicles (A) and 5 μg/mL of BSA or CD63 protein (B). The error bars represent the standard deviations from three repetitive measurements.

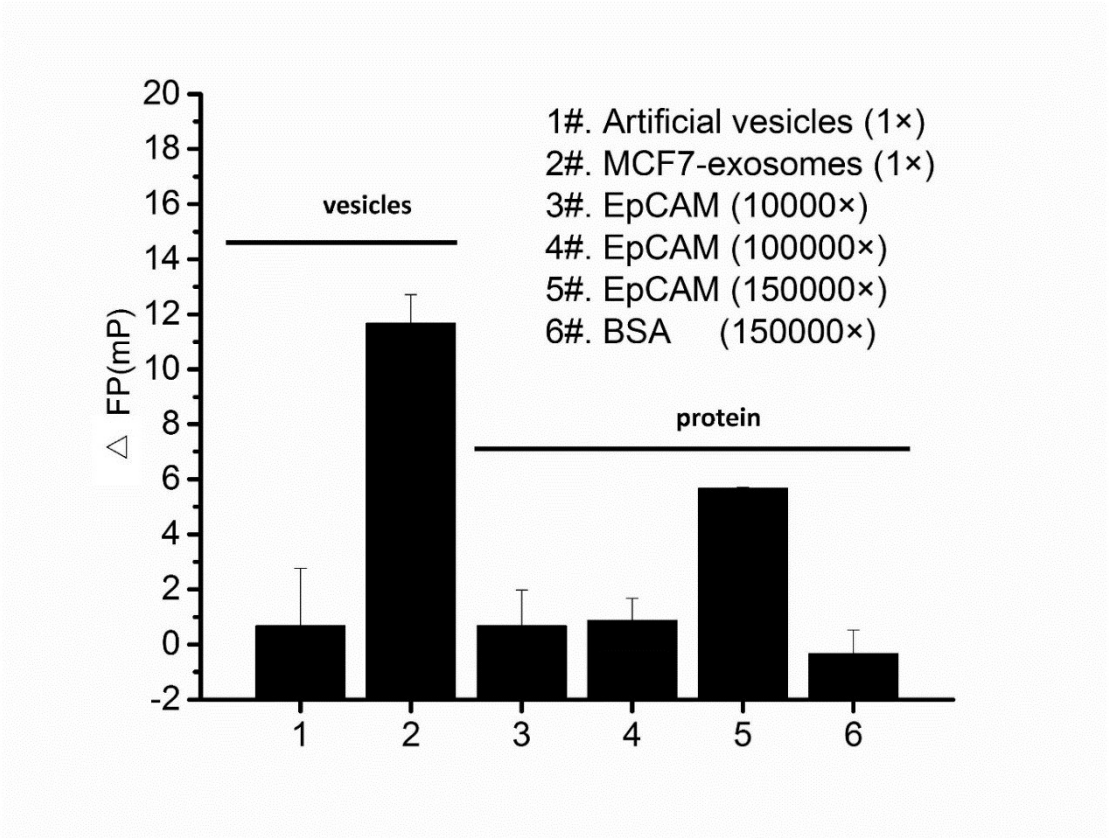

Fig. S8. The generality of our AFPExo assay. The AFPExo assay for EpCAM positive exosome detection. The selectivity of AFPExo assay for the artificial vesicles, MFC7-exosomes, EpCAM and BSA. The error bars represent the standard deviations from three repetitive measurements. The sequence of EpCAM aptamer was: 5'- Texas Red-CAC TAC AGA GGT TGC GTC TGT CCC ACG TTG TCA TGG GGG GTT GGC CTG-3'. Reaction buffer was PBS containing 1 mM $MgCl_2$. Recombinant human EpCAM protein was obtained from Sino Biological. 5nM Texas Red labeled EpCAM aptamer was incubated with artificial vesicles (5×10^5 particles/μL, 1×), MCF7-exosomes (5×10^5 particles/μL, 1×), EpCAM (0. 33 μg/mL, 10000×; 3.33 μg/mL, 100000×; 5.00 μg/mL, 150000×) and BSA (5.00 μg/mL, 150000×) at room temperature for 0.5h, separately. For Texas Red-aptamer, an excitation filter at 590 nm and an emission filter at 612 nm were used. Other conditions were the same as those of CD63 aptamer.

Our AFPExo assay showed not only a high sensitivity for the detection of exosome secreted from MCF7 cells, but also a high specificity toward EpCAM on the exosomes over artificial vesicles and free EpCAM protein. The concentration of free EpCAM in the clinical serum/plasma is reported in the ng/mL range, [12,13] which is much lower than that could be detected by the AFPExo assay. Thus, the free-EpCAM in human serum/plasma could not influence the FP signal from EpCAM-specific exosomes.

Table for the methods comparison

Table S1 Comparison of the methods for exosome detection.

Method	EVs isolation step	Special materials	Magnification step	Assay time (h)	LOD (partilces/ul)	Ref
quantum dot-based electrochemical detection	magnetic beads	CdSeQDs	dissolution of CdSeQDs	~2.5	100	[3]
electrochemical sandwich immunosensor	plate	no	second antibody	~1	200	[4]
nano-plasmonic exosome (nPLEX) sensor	plate	periodic nanohole arrays	no	~0.5	400	[5]
paper-based aptasensor	paper	UCNPs and AuNRs*	no	~0.5	1.1×10^3	[6]
copper-mediated exosome detection	magnetic beads	CuO NPs	dissolution of CuO NPs	~2	4.8×10^4	[7]
B-Chol anchor assay with enzyme-linked HCR	magnetic beads	Enzyme-linked HCR	HCR	>12	2.2×10^3	[8]
aptasensor based on DNA-capped s-SWCNTs	DC**	s-SWCNTs	no	~0.67	5.2×10^5	[9]
aptasensor based on DNA-adsorbed g-C3N4 nanosheets	DC**	g-C_3N_4 nanosheets	no	~0.5	13.5×10^5	[10]
ExoScreen	no need	photosensitizer beads ***	no	1.5-3	-	[11]
AFPExo	no need	no	no	~0.5	500	This work

* UCNPs: upconversion nanoparticles; AuNRs: gold nanorods
**DC: differential centrifugation
***AlphaLISA reagents consisted of AlphaSreen donor beads and acceptor beads)

References:

[1] J. R. Lakowicz, *Principles of Fluorescence Spectroscopy, 3rd ed.* Springer Science: New York, **2006**.
[2] B.-C. Ye,B.-C. Yin, *Angew. Chem. Int. Ed.* **2008,** *47*, 8386.
[3] K. Boriachek,M. N. Islam,V. Gopalan,A. K. Lam,N. Nam-Trung,M. J. A. Shiddiky, *Analyst* **2017,** *142*, 2211.
[4] X. Doldan,P. Fagundez,A. Cayota,J. Laiz,J. P. Tosar, *Anal. Chem.* **2016,** *88*, 10466.
[5] H. Im,H. Shao,Y. I. Park,V. M. Peterson,C. M. Castro,R. Weissleder,H. Lee, *Nat. Biotechnol.* **2014,** *32*, 490.
[6] X. Chen,J. Lan,Y. Liu,L. Li,L. Yan,Y. Xia,F. Wu,C. Li,S. Li,J. Chen, *Biosens. Bioelectron.* **2018,** *102*, 582.
[7] F. He,J. Wang,B.-C. Yin,B.-C. Ye, *Anal. Chem.* **2018,** *90*, 8072.
[8] F. He,H. Liu,X. Guo,B.-C. Yin,B.-C. Ye, *Anal. Chem.* **2017,** *89*, 12968.
[9] Y. Xia,M. Liu,L. Wang,A. Yan,W. He,M. Chen,J. Lan,J. Xu,L. Guan,J. Chen, *Biosens. Bioelectron.* **2017,** *92*, 8.
[10] Y.-M. Wang,J.-W. Liu,G. B. Adkins,W. Shen,M. P. Trinh,L.-Y. Duan,J.-H. Jiang,W. Zhong, *Anal. Chem.* **2017,** *89*, 12327.
[11] Y. Yoshioka,N. Kosaka,Y. Konishi,H. Ohta,H. Okamoto,H. Sonoda,R. Nonaka,H. Yamamoto,H. Ishii,M. Mori,K. Furuta,T. Nakajima,H. Hayashi,H. Sugisaki,H. Higashimoto,T. Kato,F. Takeshita,T. Ochiya, *Nat. Commun.* **2014,** *5,* 3591.
[12] F. Tas, S. Karabulut and D. Duranyildiz, *Mol. Cell. Biochem*, **2014**, *396*, 307.
[13] S. Karabulut, F. Tas, D. Tastekin, M. Karabulut, C. T. Yasasever, R. Ciftci, M. GÜveli, M. Fayda, S. Vatansever and M. Serilmez, *Tumor Biology*, **2014**, *35*, 8849.